

# Experimental Analysis and Simulative Validation of Dynamic Spectrum Access for Coexistence of 4G and Future 5G Systems

Florian Kaltenberger and Raymond Knopp  
EURECOM  
Sophia-Antipolis, France

Martin Danneberg and Andreas Festag  
Vodafone Chair Mobile Communication Systems  
Technische Universität Dresden, Germany

**Abstract**—5G mobile networks will very likely include features that allow for a dynamic spectrum access (DSA) in order to exploit spectrum holes of a primary system. The efficient utilization of spectrum holes with minimum impairment of the primary system requires a waveform with a very low adjacent channel leakage ratio as well as robustness to time and frequency offsets. One of the approaches for new waveforms is Generalized Frequency Division Multiplexing (GFDM), a digital multi-carrier transceiver concept that employs pulse shaping filters to provide control over the transmitted signal's spectral properties. In this paper we present experimental results that evaluate the impact of the new GFDM waveform on an existing 4G system. The 4G system was based on Eurecom's OpenAirInterface for the eNB and a commercial UE. The 5G system was emulated using the LabVIEW/PXI platform with corresponding RF adapter modules from National Instruments and TUD's GFDM implementation. The experimental results show that GFDM can be used with about 5 dB higher transmit power than a corresponding orthogonal frequency division multiplexing (OFDM) system, before any impact on the primary system is noticeable. The results from our real-time measurements were validated by simulations.

## I. INTRODUCTION

LTE-Advanced is a fourth generation (4G) mobile system that is currently being deployed worldwide. In the meantime, researchers are already thinking about a fifth generation mobile system, referred to as 5G, that should provide 1000 times more capacity and less latency than 4G systems, support for an unprecedented number of users and connected things, and ensure better energy efficiency [1]. From a physical layer (PHY) point of view, these requirements translate into higher spectral efficiency, the ability to support large and fragmented spectrum, dynamic spectrum access (DSA), and short packet transmissions with loose synchronization requirements. Orthogonal frequency division multiplexing (OFDM) and single-carrier frequency division multiplexing (SC-FDMA), which are the two waveforms used in current 4G systems do not fulfill all of these requirements, and therefore new waveforms have been proposed for 5G.

All proposed candidate 5G waveforms are generalizations of OFDM. In the case of filter-bank multi-carrier (FBMC) additional pulse-shaping filters are applied to every subcarriers [2]. Alternatively, universal filtered multi-carrier (UFMC) [3] applies filtering over multiple subcarriers, and generalized frequency division multiplexing (GFDM) [4] uses circular convolution instead of linear convolution for the filtering of the subcarriers. All of these waveforms have in

common that they reduce the adjacent channel leakage ratio (ACLR) and the peak-to-average power ratio (PAPR) compared to an OFDM system at the expense of a more complex receiver design.

In this paper we present a comparative study of GFDM, SC-FDMA, and OFDM in a cognitive radio setting. The primary system is a 4G LTE FDD system and the secondary system is a 5G TDD system that operates in the uplink frequency band of the primary system and exploits spectrum holes of a primary system. We study the performance of the primary system in presence of interference from the secondary system, which is using either GFDM, SC-FDMA, or OFDM. Both simulation and experimental results are presented. The 4G system was based on Eurecom's OpenAirInterface [5] for the eNB and a commercial UE. The 5G system was emulated using the LabVIEW/PXI Platform with corresponding RF adapter modules from National Instruments and TUD's GFDM implementation.

In previous work we have shown that GFDM is able to use the LTE master clock and the same time-frequency structure as employed in today's 4G cellular systems [6]. This capability is important to allow deployments to re-use the already developed solutions for future networks, while new and more efficient solutions are being slowly introduced. In [6] two approaches has been presented: The first GFDM setting is aligned with the LTE grid, with four LTE resource blocks to fit three GFDM subcarriers. In the other setting, GFDM acts as a secondary system to the primary LTE and two LTE resource blocks are used to fit one GFDM subcarrier. A guard band among the GFDM signal and the other resource blocks is introduced to allow for some asynchronicity between GFDM and LTE signals. In this paper, we pursue the first setting, demonstrating that GFDM can be synergetically used with the current LTE time-frequency grid, keeping the compatibility with most parameters of current generation LTE networks. While this setting requires time synchronization between the primary and the secondary system, we show that GFDM's low adjacent channel leakage exhibits benefits even when it operates without time and frequency synchronization to the primary system.

The present work extends the experimental results in [7] and [8]. Compared to the previous work, in this paper we validate the experimental results by simulation. Furthermore, the testbed setup combines the GFDM implementation operat-

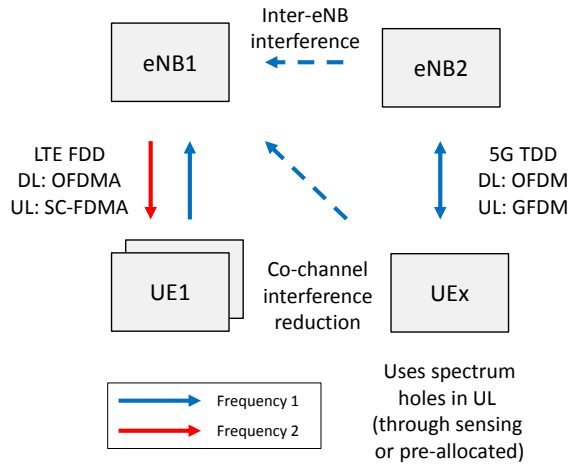


Fig. 1. Dynamic spectrum access application scenario. The primary system operates in FDD, while the secondary system operates in TDD using the UL frequency of the primary system. The inter-eNB interference can be neglected if the second eNB is sufficiently far away or indoors (typical macro/small cell HetNet scenario).

ing in the LabVIEW/PXI platform with Eurecom’s OpenAir-Interface, whereas the latter open-source environment enables flexible control of parameters and in-depth monitoring of metrics for the primary LTE system, such as layer-2 and layer-3 throughout.

The remainder of the paper is organized as follows: Section II presents the application scenario whereas Section III gives a brief overview of GFDM. The experimental setup and the testbeds used are presented in Section IV. The results from both simulation and the experiments are presented in Section V. We conclude the paper in Section VI.

## II. APPLICATION SCENARIO

The application scenario is depicted in Figure 1. The primary system (denoted by eNB1 and UE1) is a 4G LTE FDD system using OFDMA in the downlink and SC-FDMA in the uplink. The secondary system (denoted by eNB2 and UEx) is a 5G TDD system that operates in the uplink band of the primary system, exploiting spectrum holes in the primary system in order not to create any interference on the uplink to the primary eNB1. The interference on the downlink of the secondary system, i.e., from eNB2 to eNB1 can be neglected if the second eNB is sufficiently far away or indoors (typical macro/small cell HetNet scenario), which we assume here.

In Figure 2 we show a schematic of the UL spectrum showing both the primary and the secondary system. In LTE the first and the last resource block (RB) of the UL are reserved for control channels. The rest of the resources can be dynamically allocated to different UEs by the eNB scheduler. If the cell is not fully loaded it implies that some UL resources remain unscheduled and can thus be potentially used by the secondary system.

The method to detect the spectrum holes is out of the scope of this paper and the reader is referred to the literature [9]. In this work we program the eNB such that it is always leaves a predefined set of resource blocks unscheduled.

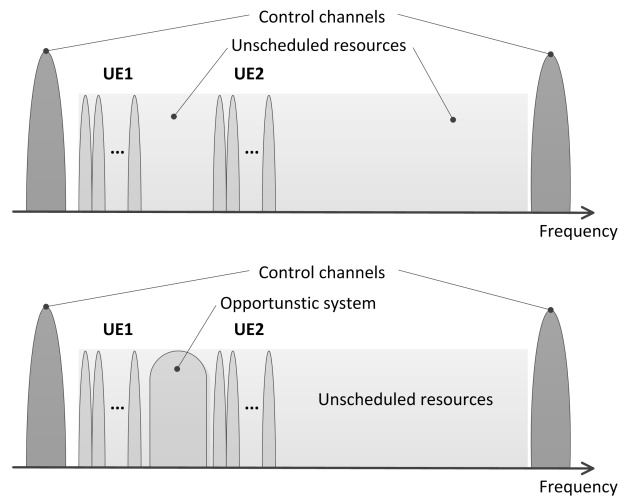


Fig. 2. Spectrum of the uplink showing the primary system and a secondary system that exploits spectrum holes.

## III. GFDM DESCRIPTION

GFDM is a multicarrier system with flexible pulse shaping. In this section, the GFDM transmitter is briefly described as a basis for the experimental work in the next section. A detailed description of the GFDM transmitter and receiver can be found in [4].

The GFDM transmitter structure is presented in Figure 3. At the input, the binary data is split up into sequences of  $KM$  complex valued data symbols. Each such sequence  $d[\ell]$ ,  $\ell = 0 \dots N - 1$ , is spread across  $K$  subcarriers and  $M$  time slots for transmission. The data can be expressed by a block structure

$$\mathbf{D} = \begin{pmatrix} \mathbf{d}_0 \\ \mathbf{d}_1 \\ \vdots \\ \mathbf{d}_{N-1} \end{pmatrix} = \begin{pmatrix} d_{0,0} & \dots & d_{0,M-1} \\ \vdots & & \vdots \\ d_{K-1,0} & \dots & d_{K-1,M-1} \end{pmatrix}, \quad (1)$$

where  $d_{k,m} \in \mathbb{C}$  is the data symbol transmitted on the  $k^{\text{th}}$  subcarrier and in the  $m^{\text{th}}$  time slot. Equation 1 represents the time and frequency resources in a GFDM block with a total number of  $N = KM$  symbols.

Consider a complex data symbol  $d_{k,m}$  of the GFDM data block. It is first up sampled by the factor  $N$ , such that the circular pulse shaping filter  $g$  can be applied. Afterwards the pulse shaped symbol is up converted by  $e^{j2\pi\frac{k}{K}n}$  to the  $k^{\text{th}}$  subcarrier. The following equation shows the modulation process which is applied at each data symbol

$$g_{k,m}[n] = g[(n - mK) \bmod N] e^{j2\pi\frac{k}{K}n} \quad (2)$$

with  $n$  denoting the sampling index. The modulo operation shifts the pulse shaping filter circularly in time. The resulting time signal  $x$  is a superposition of all modulated data symbols.

$$x[n] = \sum_{k=0}^{K-1} \sum_{m=0}^{M-1} d_{k,m} g_{k,m}[n], \quad n = 0, \dots, N - 1. \quad (3)$$

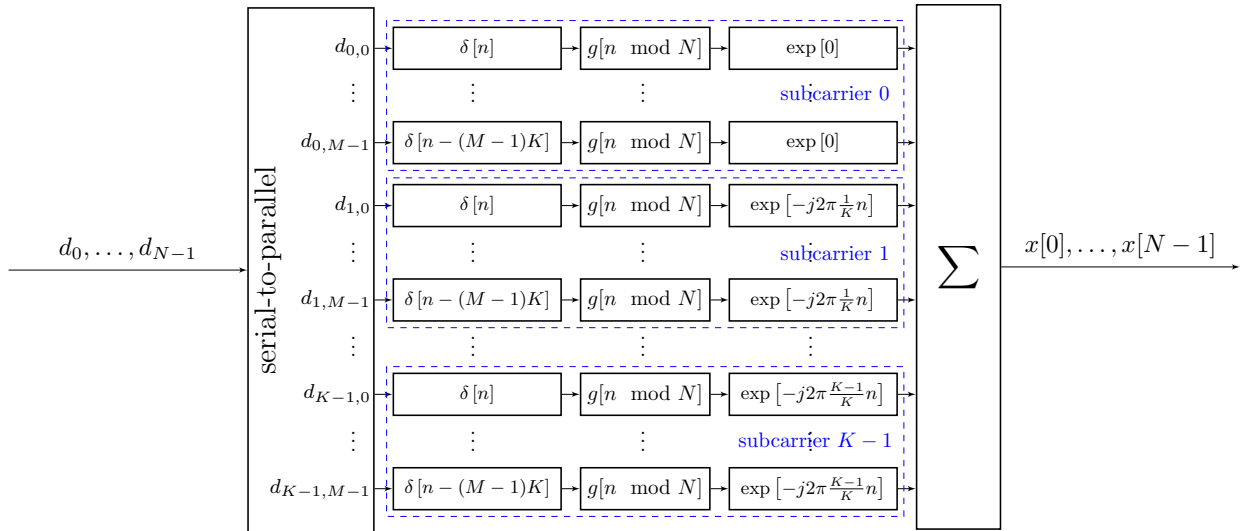


Fig. 3. GFDM transmitter system model as depicted in [4].

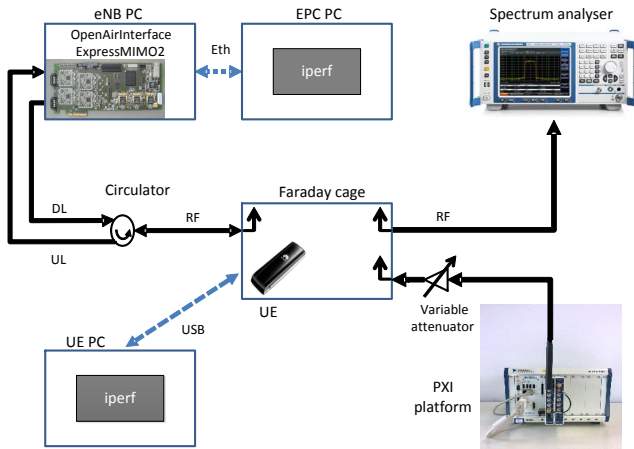


Fig. 4. Experimental setup.

The cyclic prefix (CP) is added for an entire GFDM block containing multiple subsymbols. Thus, the overhead is reduced which improves the spectral efficiency of the system.

According to the model OFDM can be seen as a special case of GFDM, where  $M = 1$  and rectangular pulse shaping is applied. Single carrier transmission is another special case, where  $K = 1$  and there is no restriction to the filter. Hence, GFDM can be thought of as a generalized case of frequency division multiplexing, where OFDM and single-carrier transmission are the two particular modes of transmission.

#### IV. EXPERIMENTAL SETUP

The experimental setup is depicted in Figure 4. The eNB of the primary system is implemented using the OpenAirInterface eNB, which consists of an off-the-shelf PC running the OpenAir4G LTE Rel 8 software modem and an ExpressMIMO2 radio card (see more details in the following subsection). The eNB is connected via Ethernet to another PC running the evolved packet core (EPC). The UE is a Huawei E398

LTE USB dongle, which is connected to a standard Windows PC. This setup allows for an end-to-end application layer connection between the Windows PC and the PC running the EPC. We use the *iperf* application to measure the throughput between these two PCs.

The secondary UE is implemented using the LabVIEW/PXI platform from National Instruments comprising the NI-FlexRIO-FPGA-Module 7965 and the RF-Transceiver-Module 5791. The transmit waveforms are generated in Matlab and transferred to a LabView program on the PXI that further transmits the waveform over RF. In order to change the power levels of the interferer, a variable attenuator is added before the antenna.

Both the primary eNB as well as the secondary UE are connected to antennas, which are placed inside a Faraday cage. The primary UE is placed entirely in the cage as well. This setup guarantees that we are not receiving any other interference and also that we are not creating any harmful interference to commercial LTE networks. Finally a spectrum analyzer is also connected to an antenna in the Faraday cage and allows us to observe both the primary and the secondary system at the same time.

The primary eNB has been configured in LTE band 7 (FDD) with a DL carrier frequency of 2.68GHz, a transmission bandwidth of 5MHz (25 RBs), transmission mode 1 (SISO), and a total output power of 0dBm. The scheduler of the eNB has been configured in such a way that it only schedules RBs 1 – 20 on the UL (RBs 0 and 24 are reserved for the control channels). Further the UL modulation and coding scheme (MCS) has been set to 8, which corresponds to QPSK modulation, and a transport block size (TBS) of 2792 bits per subframe. Since we only schedule 3 subframes out of the available 10, the total PHY layer throughput 818 kbps. Due to protocol overhead from layer 2 and layer 3, the maximum throughput at the application layer is slightly less.

The secondary system is using either an OFDM waveform or a GFDM waveform, whose parameters are given in Table I.

Parameter	Symbol	OFDM SC-FDMA	GFDM
Number of subcarriers	K	512	512
Number of active subcarriers	Kon	36	36
First active subcarrier		103	103
Bandwidth		7.68 MHz	7.68 MHz
Pulse shaping filter		n/a	Raised cosine
Roll-off factor	a	n/a	0
Symbols	M	1	15
Active symbols	Mon	1	13
CP length	Ncp	36/40	512
Blocks	B	(1+6)*2	1

TABLE I. PARAMETERS OF THE SECONDARY SYSTEM

### A. The OpenAirInterface Platform

OpenAirInterface<sup>1</sup> (OAI) is an open-source hardware/software development platform and an open forum for innovation in the area of digital radio communications. OpenAirInterface software modem comprises a highly optimized C implementation of all the elements of the 3GPP LTE Rel 8 protocol stack plus some elements from Rel 10 for both user equipment (UE) and enhanced node B (eNB). The software modem can be run in simulation/emulation mode or in real-time mode together with a hardware target. EURECOM has developed its own hardware target, called ExpressMIMO2, which supports up to four antennas and a bandwidth of up to 20MHz and a frequency range from 300MHz to 3.8GHz. Recently, OAI has also been ported to run on universal software radio peripheral (USRP) B210 platform from Ettus Research, a National Instrument (NI) company.

The current software modem can interoperate with commercial LTE terminals and can be interconnected with closed-source EPC (enhanced packet core) solutions from third-parties. Recently an open-source implementation of the EPC has also been developed at EURECOM and is now part of the Openair4G software suite. The objective of this platform is to provide methods for protocol validation, performance evaluation and pre-deployment system test. See [5] for more details.

### B. The LabVIEW/PXI Platform

LabVIEW/PXI is a Software Defined Radio (SDR) platform and a tool for rapid prototyping with real-time wireless communication systems [10]. It relies on PXI (PCI eXtensions for Instrumentation), a well-accepted interface in the test equipment and instrumentation industry. As such it provides a rugged PC based platform for use in automated test, data acquisition and many other applications. The SDR platform provides a heterogeneous environment of multi-core Windows/Linux PC and real-time operating systems running on General purpose processors (GPP) and FlexRIO FPGA modules with Xilinx Virtex-5 and Kintex-7. It can be extended by RF, Digital-to-Analog Converter (DAC) and Analog-to-Digital Converter (ADC) modules. LabVIEW is also a system design software that offers a common environment for the heterogeneous platform with hardware/software integration and an abstraction layer [11]. The SDR platform makes an ideal environment to rapidly and flexibly carry out experimental research.

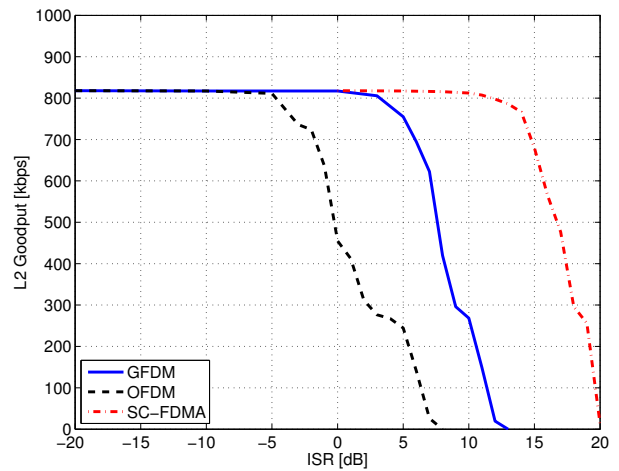


Fig. 5. Simulated layer 2 goodput of the primary system as a function of the ISR from the secondary system for the three different interfering waveforms.

## V. RESULTS

### A. Simulation

Simulations were carried out using the unitary UL simulator (*ulsim*) of OpenAirInterface and the GFDM/OFDM waveform generator, which is also used in the real experiment. The secondary waveforms were injected into *ulsim* and scaled according a predefined interference to signal ratio (ISR). The simulator implements the complete PHY plus the HARQ protocol, thus giving layer 2 goodput. Note that in this setup the interference is synchronized in time, but not in frequency, since the primary systems SC-FDMA waveform does not null out the DC carrier but instead applies a frequency offset of 7.5 kHz (half a subcarrier) to all subcarriers. We therefore also include a secondary SC-FDMA waveform in the simulation studies, which is perfectly orthogonal to the primary waveform.

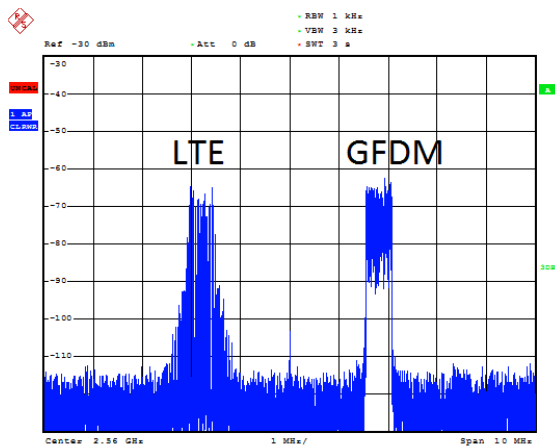
The results are shown in Figure 5. It can be seen that the fully synchronized SC-FDMA waveform performs the best, allowing an ISR up to 10 dB before taking a hit from the interfering signal. The OFDM waveform performs the worst due to its bad ACLR properties, already creating interference at -5 dB ISR. The GFDM waveform performs almost 8 dB better than OFDM due to the better ACLR values.

### B. Experiment

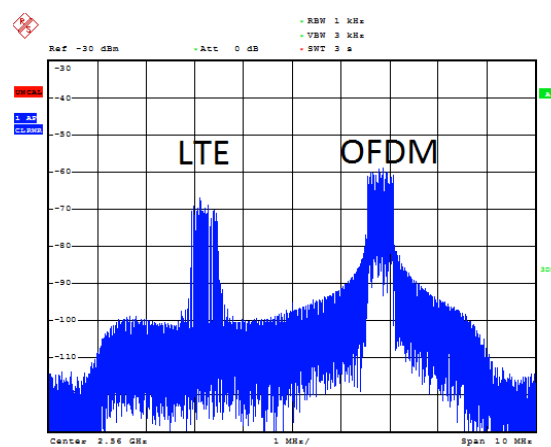
In the experimental setup we measure the goodput of the primary system after the UE has successfully connected to the eNB. To this end we use the *iperf* application to generate UDP traffic at the UE at a rate of 1 Mbps for 60 seconds. The goodput is recorded at the eNB also with the *iperf* application. Screenshots of the spectrum analyzer for both GFDM and OFDM are shown in Figure 6. The better spectral properties of GFDM are clearly visible.

In the experimental setup the UE power was measured to be -22dBm per RB and we vary the secondary TX power to achieve a given ISR. The results are plotted in Figure 7. It can be seen that SC-FDMA loses its advantage over GFDM and even performs worse than OFDM in an unsynchronized setting. The behavior of GFDM and OFDM remains approximately the same as in the simulation, but with slightly less difference

<sup>1</sup><http://www.openairinterface.org>



(a) LTE as primary system and GFDM as secondary system



(b) LTE as primary system and OFDM as secondary system

Fig. 6. Screenshots of the spectrum analyzer of primary and secondary systems, without traffic on the primary system.

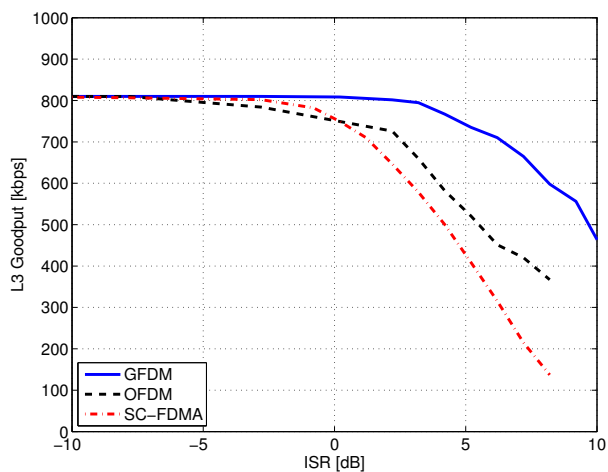


Fig. 7. Experimentally measured layer 3 goodput of the primary system as a function of the secondary transmit power for two different interfering waveforms. The goodput was measured with the *iperf* application using UDP traffic.

between them. In the experiments GFDM performs about 5dB better than OFDM.

## VI. CONCLUSION

We have shown through both simulation and real-time experiments the benefits of GFDM over OFDM and SC-FDMA in a cognitive radio setting, where GFDM is used as a waveform for a secondary system that opportunistically exploits spectrum holes in a primary LTE system. GFDM has a much lower adjacent channel leakage ratio, even when it operates without time or frequency synchronization to the primary system. Experiments were carried out using Eurecom’s OpenAirInterface and a commercial UE as a primary system and TU Dresden’s testbed based on the LabView/PXI platform implementing the secondary GFDM transmitter. The experiments show that GFDM can be used with about 5 dB higher transmit power than a corresponding OFDM system, before any impact on the primary system is noticeable. Further the experiments show rather good agreement with the simulation results.

## ACKNOWLEDGMENT

This work has been partially supported by the EU project SOLDIER (FP7-ICT-619687, <http://www.ict-solder.eu>), the EU project CREW (FP7-ICT-258301, <http://www.crew-project.eu>), and the EU Network of Excellence Newcom# (FP7-ICT-318306, <http://www.newcom-project.eu>).

## REFERENCES

- [1] J. Andrews, S. Buzzi, W. Choi, S. Hanly, A. Lozano, A. Soong, and J. Zhang, “What Will 5G Be?” *Selected Areas in Communications, IEEE Journal on*, vol. 32, no. 6, pp. 1065–1082, June 2014.
- [2] B. Farhang-Boroujeny, “OFDM Versus Filter Bank Multicarrier,” *Signal Processing Magazine, IEEE*, vol. 28, no. 3, pp. 92–112, May 2011.
- [3] G. Wunder et al., “5GNOW: Non-orthogonal, Asynchronous Waveforms for Future Mobile Applications,” *Communications Magazine, IEEE*, vol. 52, no. 2, pp. 97–105, February 2014.
- [4] N. Michailow, M. Matthe, I. Gaspar, A. Caldevilla, L. Mendes, A. Festag, and G. Fettweis, “Generalized Frequency Division Multiplexing for 5th Generation Cellular Networks,” *Communications, IEEE Transactions on*, vol. 62, no. 9, pp. 3045–3061, Sept 2014.
- [5] B. Zayen, F. Kaltenberger, and R. Knopp, *Opportunistic Spectrum Sharing and White Space Access: The Practical Reality*. Wiley, 2015, ch. OpenAirInterface and ExpressMIMO2 for spectrally agile communication.
- [6] I. Gaspar, L. Mendes, M. Matthe, N. Michailow, A. Festag, and G. Fettweis, “LTE-compatible 5G PHY Based on Generalized Frequency Division Multiplexing,” in *Wireless Communications Systems (ISWCS), 2014 11th International Symposium on*, Aug 2014, pp. 209–213.
- [7] M. Danneberg, R. Datta, A. Festag, and G. Fettweis, “Experimental Testbed for 5G Cognitive Radio Access in 4G LTE Cellular Systems,” in *Sensor Array and Multichannel Signal Processing Workshop (SAM), 2014 IEEE 8th*, June 2014, pp. 321–324.
- [8] M. Danneberg, R. Datta, and G. Fettweis, “Experimental Testbed for Dynamic Spectrum Access and Sensing of 5G GFDM Waveforms,” in *Vehicular Technology Conference (VTC Fall), 2014 IEEE 80th*, Sept 2014, pp. 1–5.
- [9] T. Yucek and H. Arslan, “A Survey of Spectrum Sensing Algorithms for Cognitive Radio Applications,” *Communications Surveys Tutorials, IEEE*, vol. 11, no. 1, pp. 116–130, First 2009.
- [10] “NI FlexRIO Software Defined Radio.” [Online]. Available: <http://sine.ni.com/nips/cds/view/plang/de/nid/211407>
- [11] “Prototyping Next Generation Wireless Systems with Software Defined Radios.” [Online]. Available: <http://www.ni.com/white-paper/14297/en/>